

Research on Engineering Structures & Materials



www.jresm.org

Research Article

Prediction of structural failure in single-story frame buildings under dynamic horizontal loading using Feed-Forward Neural Networks

Denise-Penelope N. Kontoni *,1,2,a, Ambrosios-Antonios Savvides 3,b, Vasiliki Tsotoulidi 3,c, Efthymia Michalopoulou 1,d

¹Dept. of Civil Eng., School of Engineering, University of the Peloponnese, GR-26334 Patras, Greece ²School of Science and Technology, Hellenic Open University, GR-26335 Patras, Greece ³School of Civil Engineering, National Technical University of Athens, GR-15780 Athens, Greece

Article Info

Abstract

Article History:

Received 06 June 2025 Accepted 12 Oct 2025

Keywords:

Feed-forward neural networks; Frame buildings; Dynamic failure; Finite element method; Earthquake-resistant design; Supervised learning In the presence of the evolution of computational mechanics and machine learning sciences, the formulation of estimation tools is of significant importance. In this article, the construction of Feed-Forward Neural Networks is presented for the estimation of failure load, failure time, and corresponding peak structure displacements, velocities and accelerations. The dataset was obtained from the computational nonlinear dynamic failure of a single-story building. It has been demonstrated that the supervised learning procedure has converged rapidly, at 4 epochs, and with a small mean squared error, namely about 1%. Moreover, the correlation between the outputs and targets of all subsets of the initial dataset vector is very strong. Following the model's reliability, it has been proven that the presence of resonance is making significant amplifications to the response of the structure, in the order of magnitude of the theoretical value of the dynamic amplification factor of 10 for sinusoidal waves. Ultimately, the formulated Networks comply with the physical constraints and are reliable for estimations that will assist in to design of earthquake-resistant infrastructures.

© 2025 MIM Research Group. All rights reserved.

1. Introduction

Dynamic failure and its triggering factors are considered of paramount importance in the Civil Engineering discipline. In the older days, the researchers could only a posteriori determine the influencing parameters of a failure, usually after an earthquake event [1-4]. This kind of scientific literature was helpful in order to documenting, categorizing, and determining the major governing factors in order to obtain a failure. Earthquake accelerations and major period in relation to eigenperiod, infrastructure intrinsic vulnerability, soil, and topographical resonance are some of the common key factors to set an infrastructure beyond repair. Nowadays, with the evolution of computer science and computational mechanics disciplines, scientific publications are substantial in number and provide some a priori investigations [5-6]. To this extent, the recent literature focuses on predicting the failure mode and investigating the major vulnerabilities of a known structure prior to known seismicity. Moreover, the type of failure may also be predicted. Determining if a brittle or ductile failure type occurs is very important for enhancing security and complying with modern regulations of design that dictate the ductile failure of materials and structures.

*Corresponding author: kontoni@uop.gr; kontoni.denise@ac.eap.gr

^aorcid.org/0000-0003-4844-1094; ^borcid.org/0000-0002-6553-0091; ^corcid.org/0000-0002-2132-0850;

dorcid.org/0009-0004-9169-7233

DOI: http://dx.doi.org/10.17515/resm2025-950st0606rs

Res. Eng. Struct. Mat. Vol. x Iss. x (xxxx) xx-xx

In recent years, a vast developing scientific field is Machine Learning and its practical usage in all disciplines of science and all different aspects of engineering [7-28]. The most prominent development occurred from 2000 onward, since the evolution of computer science was offering the infrastructure that was adequate to compute an enormous number of calculations in a very short time interval. The presentation of Physics Informed Neural Networks (PINNs), namely, an accumulation of physical problem data and the idea of a model construction for estimating this phenomenon in a generalized way. With PINNs, many scientists and engineers have developed a numerical tool to overcome computational or experimental procedures. Models that estimate the materials stress-strain law, from composite materials to geomaterials, are made from PINNs. Other machine learning models constructed estimate the response of systems of importance in every scientific subfield, such as buildings. Regarding earthquake engineering and dynamic failure, the number of scientific publications that have employed machine learning theory is still evolving. From the literature accumulated, it has been demonstrated that different ways of dataset construction have been used. Data from real structures, experimental data, and some computational studies have been performed, and the data matrices have been employed. Afterward, different ways of Machine Learning models have been employed, such as the particle swarm optimization, the genetic algorithms optimization schemes, or Bayesian inference methods. All of these works have given models of substantial reliability and can contribute to engineering estimations of response for physical systems.

In this work, a model that estimates the main parameters at failure of a single-story building subjected to a horizontal dynamic load is presented. The model is formulated through a Feed-Forward Neural Network architecture. The horizontal dynamic load is sinusoidal with an excitation period equal to the structure's eigenperiod. The input parameters of the model are the frame height H, the frame length L, the Young Modulus E, the yield stress σ_v , and the eigenperiod of the structure T. The output parameters of the model are the failure load P_0 , the time of the failure t_0 , the maximum displacement d_{max} of the frame at failure, the corresponding maximum velocity v_{max} , and the corresponding maximum acceleration a_{max}. The dataset matrix has a size of 1440. The dataset was obtained with analyses in ANSYS (ANSYS, Inc.) and Open-Source computational mechanics MSolve. The analysis was employed by Fiber Beam Force-Based Elements. In addition, the failure of the structure was determined as if a percentage of the total element fibers failed, which means it exceeded the maximum allowed strain. Finally, after the accumulation of the dataset matrix, a neural network model was obtained with the aid of the MATLAB neural network toolbox (The MathWorks, Inc.). Two hidden layers with 64 Neurons each were selected as the architecture. The activation functions are the sigmoid function for all layers except the output layer, and the pure linear to the output layer. The error metric was the Mean Squared Error (MSE), and the early stopping was employed to avoid overfitting. The outline of this article is the following. Initially, a brief presentation of the dynamic failure and its particular determination employed is given. Then, the Machine Learning framework adopted in the present study is given. Subsequently, the practical part of this work follows. The definition of the problem and the presentation of the results will be provided with the relative discussion. Finally, concluding remarks with future work will be provided.

2. Dynamic Failure of Structures - Definition and Properties

Dynamic loading and the corresponding failure are a complex phenomenon. Its definition is a matter of discussion among the engineers. It is a common point of view that failure under any circumstances occurs when the physical system has exceeded its load-bearing capability. While this is a comprehensive phase, defining the stress-strain or the force-displacement pair that represents this capability is disputable. Many approaches have been proposed regarding this. Some of them are displacements of certain places of a structure, not to exceed a defined value, obtained from experimental or in situ experience. Moreover, an inter-story drift maximum value may also be incorporated. In addition, in computational models, the stiffness reduction over a specified threshold, like 5% of the initial stiffness, could also be employed. Finally, a selection of a number of Gauss integration points that would exhibit softening, namely a negative plastic hardening modulus, is also an alternative among others.

The dynamic loading of a structure may be induced by an earthquake, machine oscillations, or other external forces. Its mathematical formulation as a multi-degree-of-freedom system is given as;

$$M\ddot{u} + C\dot{u} + F_{int} = P \tag{1}$$

where P is the external force vector as a function of time, M, C, F_{int} stand for the classical mass, damping matrices, and internal forces vector obtained by the standard FEM and Newton-Raphson iterative methods. A common function of P is the following $P = P_0 \sin(\omega t)$, where P_0 and ω are the peak load and frequency of excitation, respectively.

The dynamic loads, from the qualitative point of view, compared to the static loads, are more detrimental in general. That is explained because the momentum of the seismic energy causes damages as a result of the inertia forces. Moreover, a resonance may be obtained in dynamic loading. This resonance may occur when the natural frequency of the building equals the excitation frequency. However, soil or topographical factors may also result in resonance. Thus, the displacements and damages may be increased in regard to static loading. From the computational point of view, a dynamic nonlinear analysis is a more stable and convergent process in comparison to a static nonlinear analysis. This is a consequence of the mass matrix participation in the integration of the equation of motion. It has a contributing factor analogous to the inverse square of the load step; thus, the solution is easier to be obtained in relation to the static nonlinear analysis.

In this work, a dynamic failure analysis of a single-story building is performed for various geometries and material parameters. The dynamic equation of (1) is solved for the resonance of each structure that is assumed, namely, when the eigenperiod and period of excitation are the same. The elements used are the fiber beam force-based proposed by Spacone et al. [29]. The failure in this work was defined as if to an element more than 50% of the total fibers have failed. Failure of a fiber is defined when its strain exceeds its maximum allowed value of 10%.

3. Feed-Forward Neural Networks — Architecture and Supervised Learning

The feed-forward neural network architecture (FNN) is the set of units, named neurons, allocated to several groups, called layers. The aforementioned structure is described as follows. Consider an FNN comprising n_l layers, where each layer comprises n_n neurons. All layers, with the exception of the input layer, are given a weight matrix W and a bias vector b, which constitute their importance in the FNN. All these matrices comprise the model's adjustable hyperparameters. In each layer, a function that relates it to the next layer is assigned. This function is called the activation function, and here it is symbolized as A. In Fig. 1, a schematic representation of an FNN comprising one hidden layer is given. The layer of the input represents the set of the following variables: the frame height, the frame length, the yield stress, the Young Modulus, and the eigenperiod of the structure. The layer of the output represents the set of the following variables: peak load at failure, the time that this failure occurs, the maximum displacement, the maximum velocity, and the maximum acceleration of the structure. The implementation of an FNN for a specific layer i, given below;

$$z_i = A(W_i z_{i-1} + b_i)$$
, $i = 1, ..., n_l$ (2)

Equation (2) simply denotes that an FNN is a mapping function from the previous layer to the next one, and in a broader view, from input to output using the set of the analogous activation functions.

The FNN hyperparameter determination is performed via supervised learning. Supervised learning dictates that the FNN is provided data samples, comprising an input and a target (flag) value, and then the parameters are altered in order to minimize the divergence from an error metric, which connects output and target values. The most common error metric is the Mean Squared Error (MSE), which is given below:

$$MSE = \frac{1}{N_{data}} \sum_{i=1}^{N_{data}} (output_i - target_i)^2$$
(3)

In general, the optimization of equation (3) refers to a non-convex objective function; thus, the solution methods are restricted to quasi-Newton schema. The FNN architecture is the most simple and prominent in the field of machine learning. It can provide, in many cases, accurate and reliable modeling. Unlike recurrent neural networks, they are not requiring training loops from outputs already accumulated. Consequently, the model formulation is faster and easier to be retrained.

In this work, the FNN architecture is used for the formulation of a surrogate model that estimates the dynamic failure of a single-story building under a dynamic horizontal force of a sinusoidal nature, with a frequency the same as the eigenfrequency of the structure. Two hidden layers with 64 Neurons each were selected as the architecture. As the error metric, the MSE function of equation (3) was selected. The input variables are the frame height, the frame length, the yield stress, the Young Modulus, and the eigenperiod of the structure. The output layers are the peak load at failure, the time that this failure occurs, the maximum displacement, the maximum velocity, and the maximum acceleration of the structure.

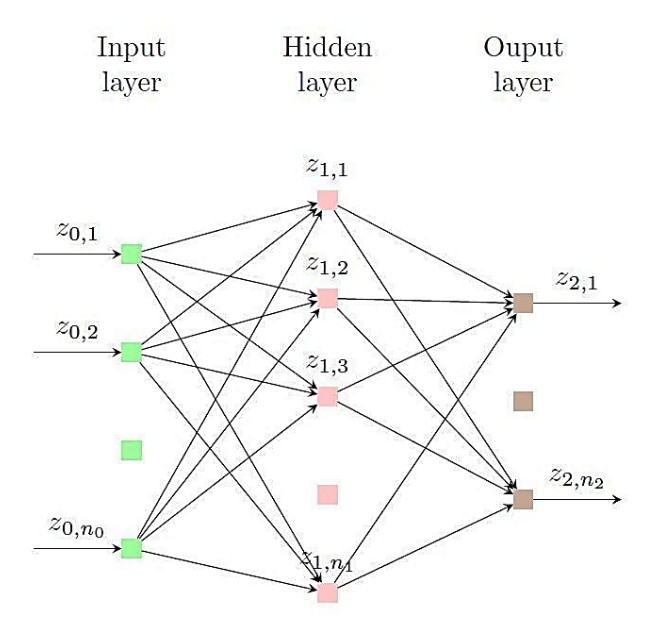


Fig. 1. A setup of a feed-forward Neural Network containing a single hidden layer

4. Model Hyperparameter Determination and Activation Function

One important aspect of every machine learning modeling formulation is the model's hyperparameter determination. The definition of the weight and bias matrices in order to minimize the error function is a non-trivial task. Many methods are proposed. A prominent choice is the Levenberg-Marquardt algorithm, namely the optimization of the square root of the sum of the squares of a vector. Another proposal is the Adam optimizer method, namely the implementation of the optimization scheme named Adaptive Moment Estimation, which is an adaptive learning method algorithm using gradient history. An alternative method similar to Adam is the Tree Parzen Estimator, which is a Bayesian inference optimization method.

The selection of the activation function, namely the relation between a previous and a subsequent layer, is very decisive for the reliability of the feed-forward neural network. In the precedent years, several functions have been used and proven to be of significant value. Initially, all the linear-type functions have been proposed especially for the relation between the last hidden layer and the output layer. Pure linear and Rectified Linear Unit functions can be useful, depending on the physical or other constraints that should be applicable. Rectified Linear Unit is the linear function for positive input, which is not differentiable at zero. Other proposals of activation functions are the logistic or alternatively sigmoid function, used in language recognition models, and the Gaussian Error Linear Unit (GELU), which is more specialized for random models or nature interpretation models [30-32].

An activation function should comply with the following propositions:

- Universal Approximation Theorem: When the activation function is nonlinear, a FNN with two layers is proven to be a structure that results in an accurate and reliable model.
- Finite Activation Range: For a finite range of an FNN, gradient-based training algorithms are more robust, because pattern recognition schema significantly affects a limited amount of weight factors.
- Infinite Activation Range: For an infinite range of an FNN, training is more effective because the pattern recognition schema significantly affects the majority of the weight factors.

A sigmoid function is convex for values less than a particular point, and it is concave for values greater than that point: in many of the examples here, that point is 0. The logistic or sigmoid activation function is stated as follows:

$$Sigmoid(x) = \frac{1}{1 + e^{-x}} \tag{4}$$

In this work, the activation function selected is the sigmoid nonlinear function for all layers except the output layer. The output layer has the pure linear function. The determination of weight and bias matrices is attained through the Levenberg-Marquardt algorithm since the Error function is the Mean Squared Error (MSE).

5. Numerical Application - Formulation of A Neural Network Model Estimating the Dynamic Failure of a Single-Story Building Under a Horizontal Dynamic Sinusoidal Load

The aforementioned theoretical framework is applied to the single-story structure of Figs. 2, and 3. In Fig. 2, the structure is presented alongside the dynamic horizontal load applied at the top of the structure. In Fig. 3, the cross-section adopted for all beam elements is shown. The structure was simulated with the Euler-Bernoulli fiber beam force-based. The frequency excitation of the dynamic load in all cases was the same as the frequency of the structure, that is $\overline{\omega} = \omega$. The structure was excited by altering the peak load until failure was obtained. Failure was defined as if to an element more than 50% of the total fibers have failed. Failure of a fiber is defined when its strain exceeds its maximum allowed value of 10%. Each fiber has the constitutive material model of linear-elastic and linear-hardening uniaxial law with a hardening modulus equal to 10% of the Young's Modulus. The analyses were performed in the ANSYS software (ANSYS, Inc.) and the opensource computational mechanics code MSolve of the Institute of Structural Analysis of the School of Civil Engineering of the National Technical University of Athens (NTUA). A parametric study was performed for the following values: the frame height H (m), the frame length L (m), the Young Modulus E (GPa), the yield stress σ_v (MPa), and the eigenperiod T (s). Specifically, the selected values for H were 3, 3.5 and 4 (m), for L were 3, 4, 5, 6 and 7 (m), for E were 200, 210, 250 and 300 (GPa), for σ_v were 200, 275, 300 and 355 (MPa), and for T were 0.05, 0.1, 0.25, 0.5, 0.75 and 1(s).

Table 1. Selected values for the input parameters. All input vectors were generated as Cartesian product of the selected values

Parameter	Selected Values
H (m)	3, 3.5, 4
L (m)	3, 4, 5, 6, 7
E (GPa)	200, 210, 250, 300
σ _y (MPa)	200, 275, 300, 355
T (s)	0.05, 0.1, 0.25, 0.5, 0.75, 1

The aforementioned selected values are depicted in Table 1, and all input vectors used for the analyses were made through the Cartesian product of the selected values. Subsequently, a total of 1440 analyses were performed, and the values of failure load P_0 , the time of the failure t_0 , the maximum displacement d_{max} of the frame at failure, the corresponding maximum velocity v_{max} , and the corresponding maximum acceleration a_{max} were accumulated. Subsequently, the dataset matrix

was obtained, and the FNN training procedure was performed. The FNN formulated had 5 input variables, namely H, L, E, σ_y , T, and 5 output variables, namely, P_0 , t_0 , d_{max} , v_{max} a_{max} . The FNN architecture comprises of two hidden layers with 64 neurons in each layer. The activation functions are the sigmoid relation of equation (4) for all layers apart from the output.

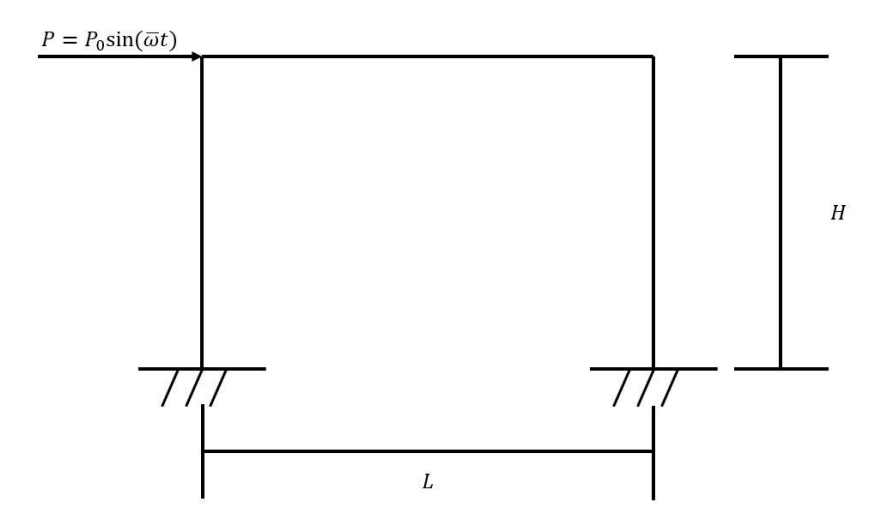


Fig. 2. A single-story building, analyzed in this work for dynamic failure

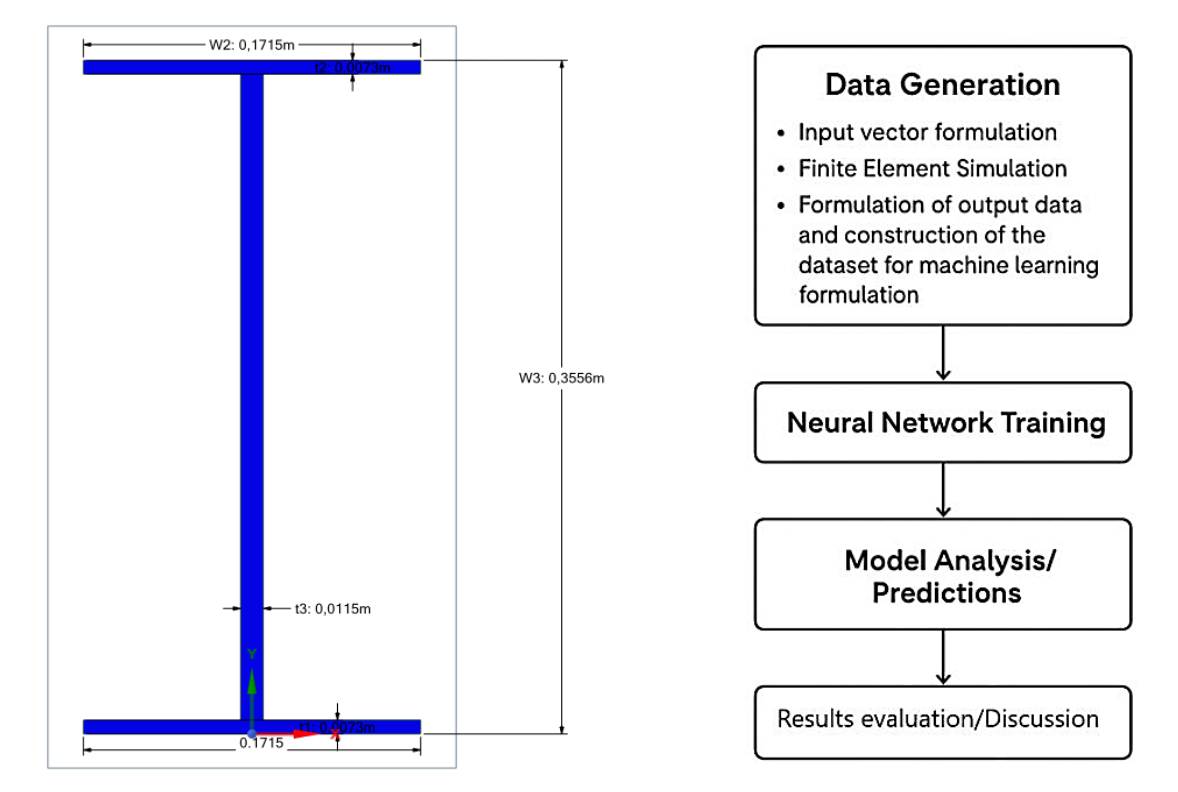


Fig. 3. The cross-section of the single-story building

Fig. 4. Workflow analysis of the present work

The output layer is activated through pure linear relation. The error metric was performed through the MSE error function of equation (3). The model hyperparameter determination is through the Levenberg-Marquardt algorithm, which is focusing on minimizing the objective function of the square root of the sum of the squares. The initial dataset matrix was subdivided into a training subset, a validation subset, and a test subset. These have sizes in the percentage of the total dataset matrix 70%, 15%, and 15% respectively. The subset indices were selected in a pure random way. In addition, a normalization of each subset was done in order to assist the supervised learning procedure to converge faster and provide a more reliable model. Finally, in order to avoid overfitting, the usage of early stopping is employed in order not to obtain too small MSE in training

and then the model to lose its generality. A schematic representation of the analysis workflow performed in this work is given in Fig. 4.

6. Results and Discussion

The results of this work are presented hereinafter. The following Figures are given: performance plot of the supervised learning (Fig. 5), and regression plots between outputs and targets (Fig. 6), for all dataset matrices (overall dataset, training, validation, and test subsets). Moreover, the error histogram is given (Fig. 7), and the statistical details of the analysis are presented (Fig. 8). Finally, an illustrative representation of the network is given for a selection of representative values of E=210 GPa, σ_y =275 MPa, and two different eigenperiods T=0.1 and T=1 s (Figs. 9-13 and Figs. 14-18). From the results presented, several important conclusions can be drawn regarding the network reliability and practical significance. The convergence analysis gives an insight into the model's accuracy. The MSE provided at the end of supervised learning is very small, namely 0.0145, and it is obtained for epochs-iterations in the order of magnitude of 10. Consequently, the model is reliable and easily adjustable to more computational or experimental data. Moreover, overfitting is avoided since the MSE curves in the validation and test subsets are practically constant for the number of epochs required for convergence in training.

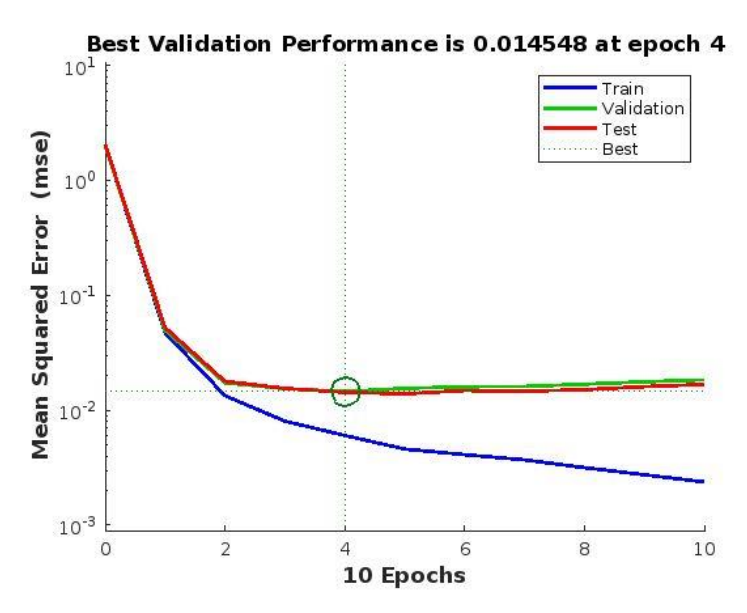
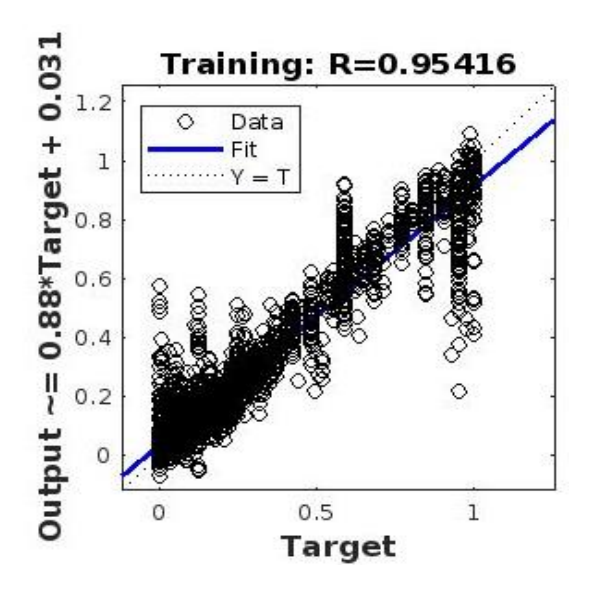
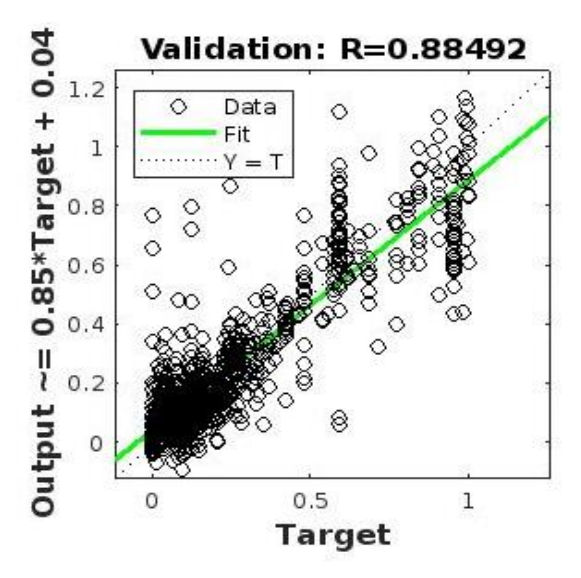


Fig. 5. Performance plot of the supervised learning





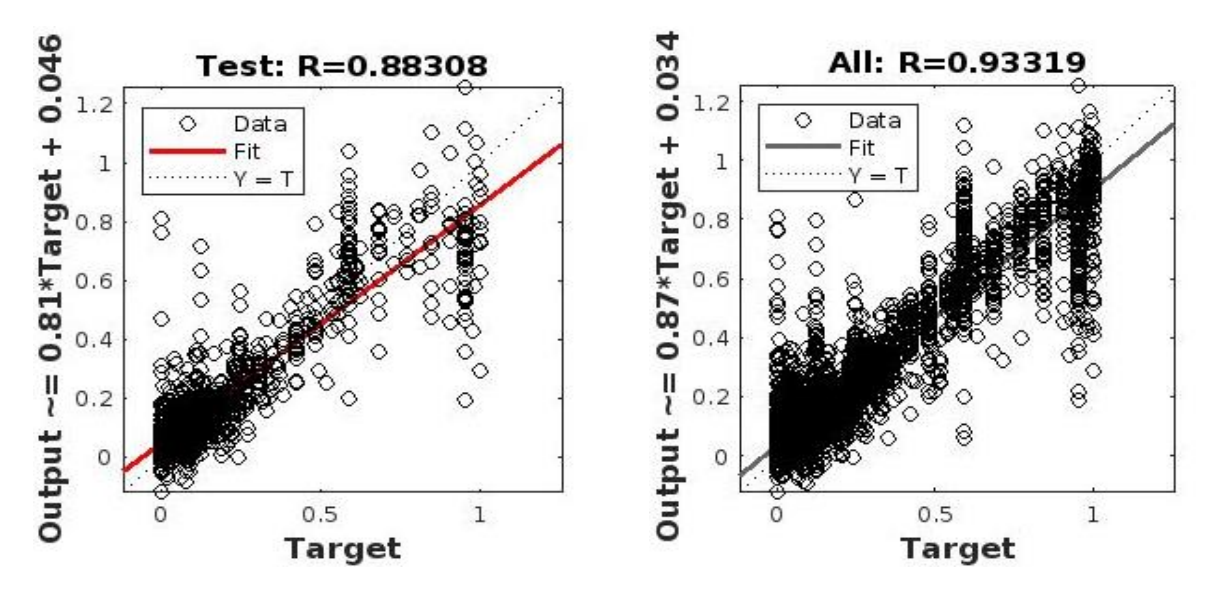


Fig. 6. Regression plots of the outputs and targets for the training subset (upper left), validation subset (upper right), test subset (lower left), and total dataset (lower right)

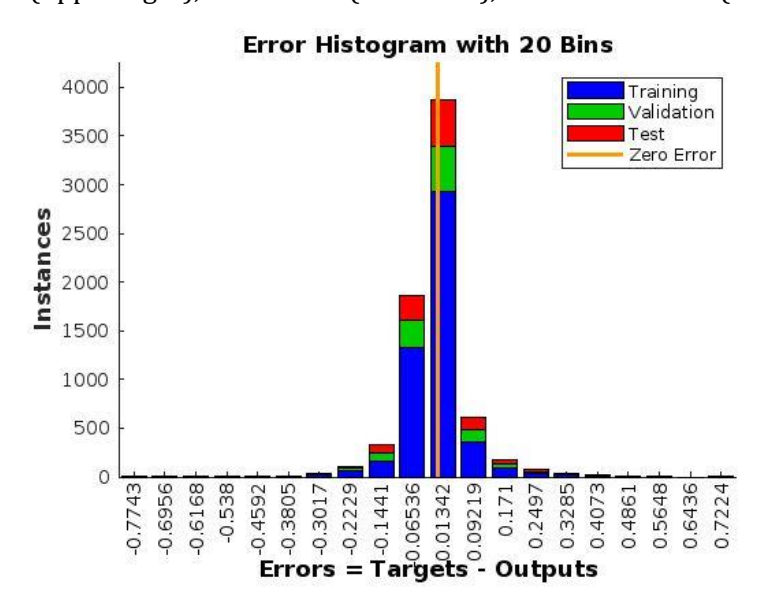


Fig. 7. Error histogram

Moreover, the error distribution is practically normal, and the mean value is very close to zero. This attribute, in combination with the fact that the samples of subsets were selected in a random way, leads to the conclusion that the error estimations are acceptable and fairly distributed. The correlation between outputs and targets in all subsets and the total dataset is considered as strong since all the correlation coefficients tend to unity. For the training subset, the correlation is estimated as 0.954, which is considered as very strong. Moreover, there is an observation of a small negligible slope that indicates that the model slightly underestimates the targets. For the validation subset, the correlation is estimated as 0.884, which is considered as very strong, however, smaller than the training subset. In addition, a small negligible slope is evident, which indicates that the model slightly underestimates the targets. For the test subset, the correlation is estimated as 0.883, which is considered as very strong, however, smaller than the training subset and practically the same as the validation subset. Again, a small negligible slope that indicates that the model slightly underestimates the targets is evident. Most importantly, the total dataset has a reliability coefficient of 0.933, which is a very strong overall coefficient of correlation that dictates that the total supervised learning is successful. The slight underestimation of the outputs in relation to targets is seen in the overall dataset. However, this would result in more conservative estimations. Thus, the model is substantially reliable and on the side of safety.

Unit	Initial Value	Stopped Value	Target Value
Epoch	0	10	1000
Elapsed Time	-	00:00:24	-
Performance	2.04	0.00238	0
Gradient	4.08	0.0102	1e-07
Mu	0.001	1e-05	1e+10
Validation Chec	ks 0	6	6

Fig. 8. Statistical metrics of the supervised learning

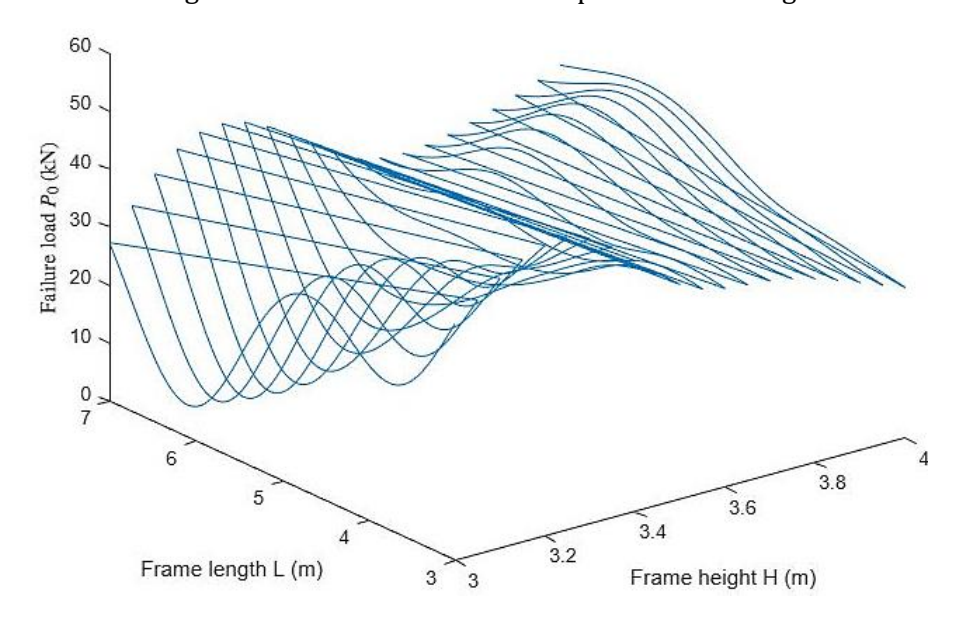


Fig. 9. Neural Network Prediction for failure load. Values for E=210 GPa, σ_y =275 MPa and T=0.1s

Regarding training parameters that concern the supervised learning process itself, it is initially observed that the 6 checks of the validation set were verified, i.e., the values estimated by the network in the validation set are close to the corresponding data values. Additionally, the slope of the performance plots during convergence is sufficiently small. The value of Mu, depicted in Fig. 8, is substantially small. This value controls the weight, and bias matrices update when the supervised learning is taking place. If this value exceeds a threshold, it is an indication that the learning rate could not be better. This is not happening in this learning, but it was proven not to be necessary since the validation checks were passed. The training was performed through Levenberg-Marquardt, which, apart from the minimization of the MSE, is a method of the unconstrained optimization problem. Since the physical problem analyzed in this work complies with error estimations with the aforementioned error metric, it is natural that this optimization algorithm is providing fast convergence and reliable optima, namely model hyperparameters.

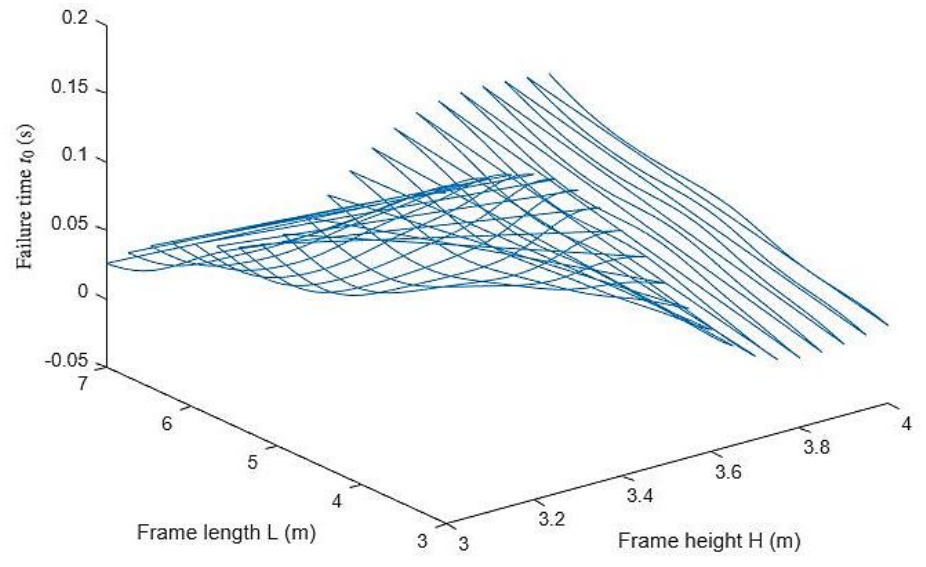


Fig. 10. Neural Network Prediction for failure time. Values for E=210 GPa, σ_y =275 MPa and T=0.1 s

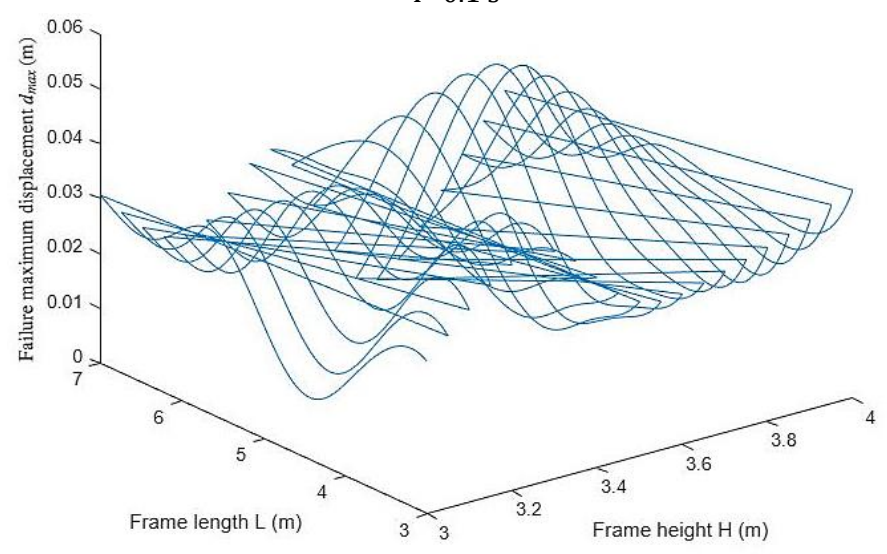


Fig. 11. Neural Network Prediction for failure maximum displacement. Values for E=210 GPa, $\sigma_{v}{=}275$ MPa and T=0.1 s

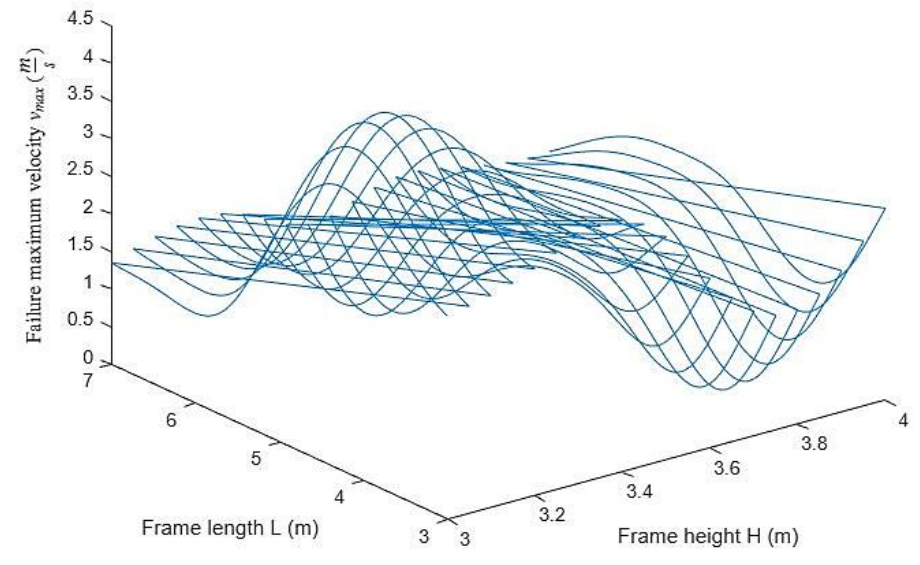


Fig. 12. Neural Network Prediction for failure maximum velocity. Values for E=210 GPa, $\sigma_y{=}275$ MPa and T=0.1 s

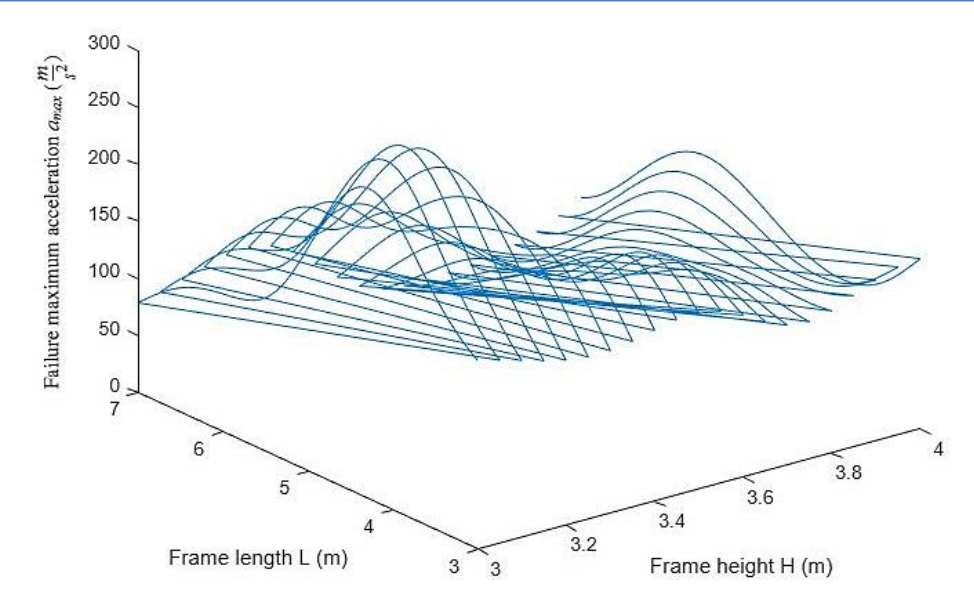


Fig. 13. Neural Network Prediction for failure maximum acceleration. Values for E=210 GPa, $\sigma_y{=}275$ MPa and T=0.1 s

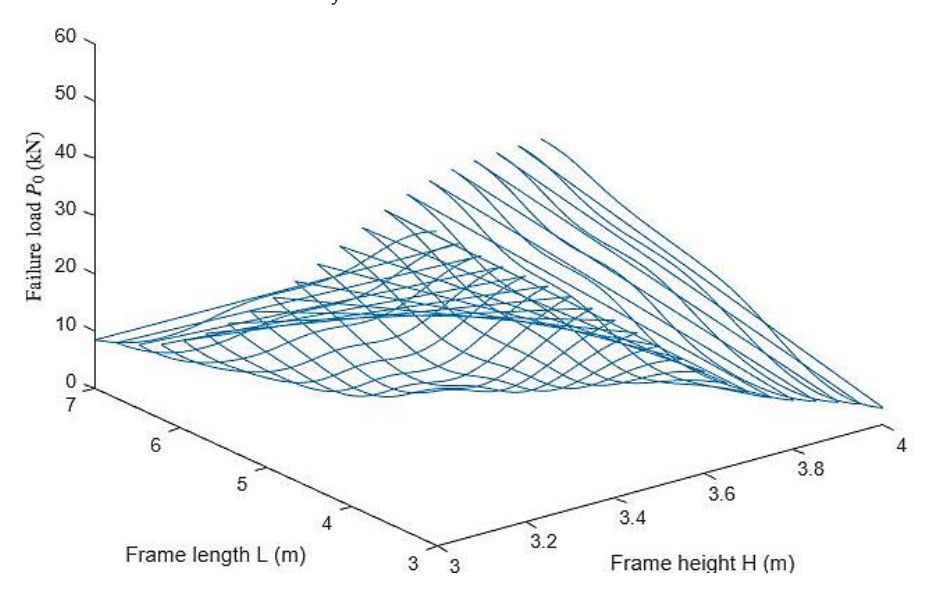


Fig. 14. Neural Network Prediction for failure load. Values for E=210 GPa, σ_y =275 MPa and T=1 s

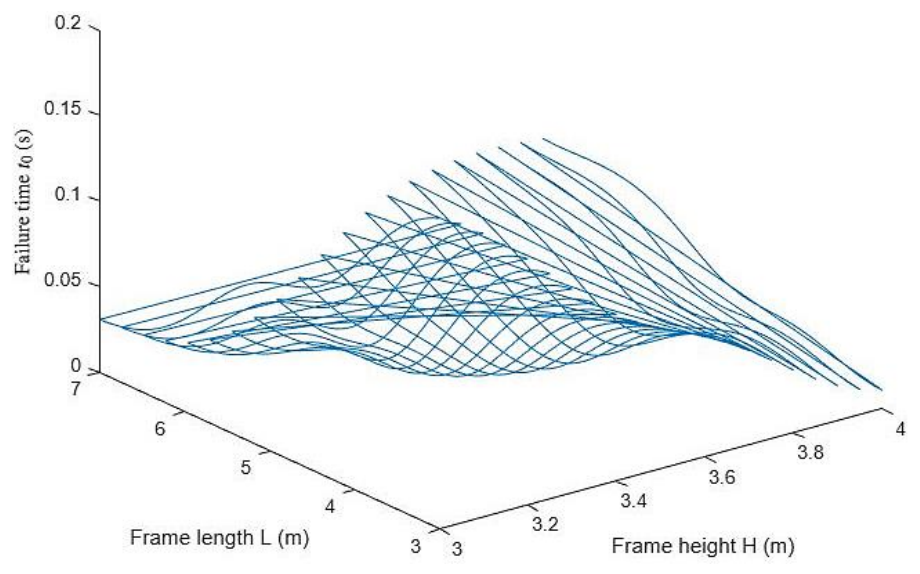


Fig. 15. Neural Network Prediction for failure time. Values for E=210 GPa, σ_y =275 MPa and T=1 s

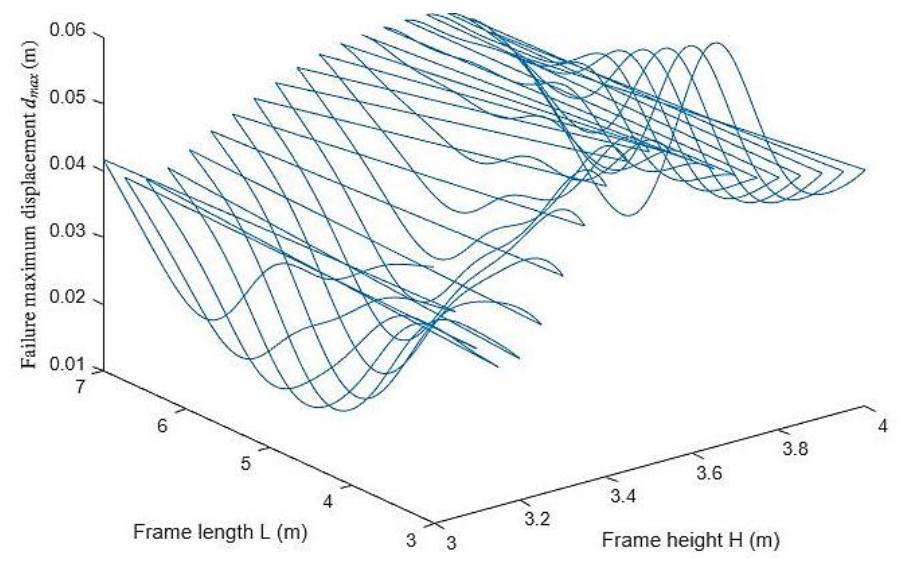


Fig. 16. Neural Network Prediction for failure maximum displacement. Values for E=210 GPa, σ_y =275 MPa and T=1 s

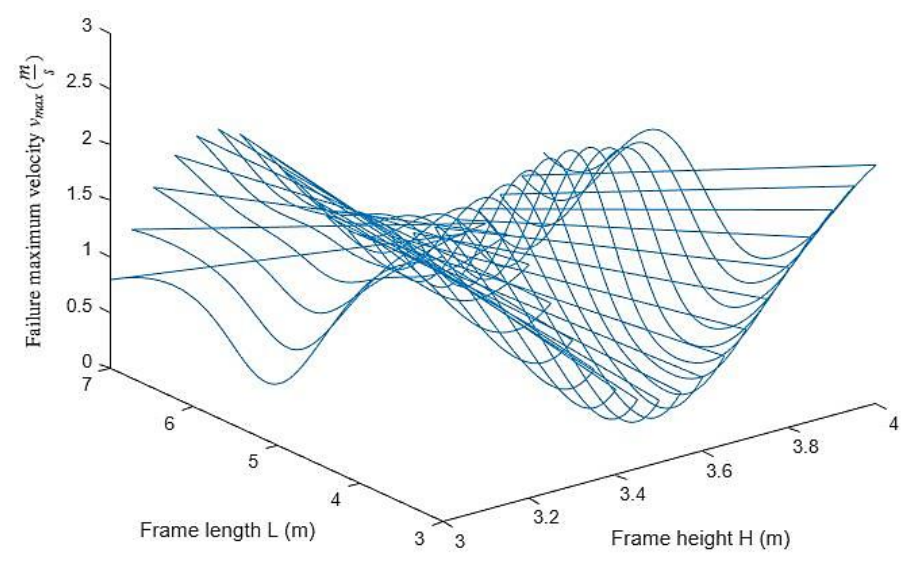


Fig. 17. Neural Network Prediction for failure maximum velocity. Values for E=210 GPa, σ_y =275 MPa and T=1 s

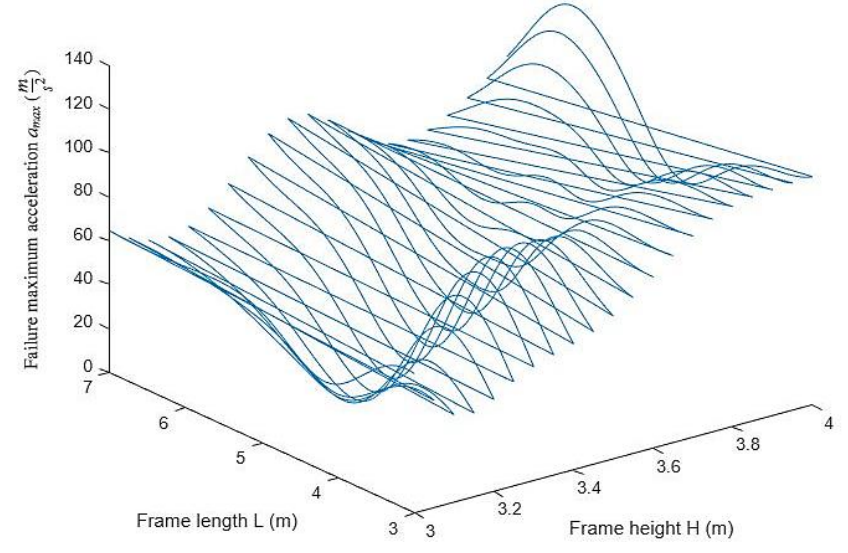


Fig. 18. Neural Network Prediction for failure maximum acceleration. Values for E=210 GPa, σ_y =275 MPa and T=1 s

The practical significance of the proposed machine learning modeling is enlightened hereinafter by presenting the selection of the representative material parameters, as well as two prominent eigenperiods for stiff and compliant structures, and the model predictions in schematic representation. As portrayed in Figs. 9-13, the network prediction for a relatively high-frequency excitation (T=0.1 s) gives values for the failure load between 5 and 50 kN. The shape of the curves is smooth and not with steep slopes. Therefore, the failure load for small changes in the geometry does not alter notably. In addition, the maximum values of the load are found at small values of the column height, as expected, since there the stiffness is greater. The network prediction for a relatively high-frequency excitation (T=0.1 s) gives values for the failure time between 0.02 and 0.15 s. The largest value of the time is found at the average value of the column height and decreases at more extreme values. The slopes are relatively steep; therefore, the difference in time can be significant for small differences in geometry. This time is however relatively short and leaves little room for escape from the structure. The network prediction for a relatively high-frequency excitation (T=0.1 s) gives values for the maximum failure displacement between 0 and 0.06 m. The largest values of the displacement are found at the largest values of beam and column lengths, as expected due to lower stiffness. The curve is not truly monotonic, but the areas where this pattern is not evident are relatively limited, and it is practically verified that the longer the lengths, the larger the failure displacements. The network prediction for a relatively high-frequency excitation (T=0.1 s) gives values for the maximum failure velocity between 1.5 and 4 m/s. The maximum values are found at the smallest values of column length and high values of beam length. The curve is not truly monotonic. However, the minimum values are found at the largest values of column length and smaller values of beam length. Therefore, in principle, the stiffest system is more likely to have a reduced maximum velocity. Therefore, it is not the length of the beams or columns that is the criterion, but the combination of these expressed by the stiffness of the system. The network prediction for a relatively high-frequency excitation (T=0.1 s) gives values for the maximum failure acceleration between 75 and 225 m/s². It is noted that these displacements are nodal and pointlike, so they may have an increased value. In fact, these are located spatially slightly lower than the top of the columns. The maximum values are achieved when the height of the frame, i.e., the columns, is 3.2 m. Therefore, for a rigid structure, the predictions are maximized. This is a result of the resonance because the rigid structure has a low eigenperiod value, as does the excitation.

As depicted in Figs. 14-18, the network prediction for a relatively low-frequency excitation (T=1 s) gives values for the failure load between 10 and 45 kN. The shape of the curves is smooth and not with steep slopes. Therefore, the failure load for small changes in the geometry does not alter significantly. In addition, the maximum values of the load are found at small values of the column height, as expected, since there the stiffness is greater. The network prediction for a relatively low-frequency excitation (T=1 s) gives values for the failure time between 0.04 and 0.15 s. The largest value of the time is found at the average value of the column height and decreases at more extreme values. The slopes are relatively steep, so the difference in time can be significant for small differences in geometry. However, this time is relatively short and leaves little room for escape from the structure.

The network prediction for a relatively low-frequency excitation (T=1 s) gives values for the maximum failure displacement between 0 and 0.065 m. The largest values of the displacement are found at the largest values of beam lengths and mainly columns, as expected due to lower stiffness. The curve is not truly monotonic, but the areas where this pattern is not evident are relatively limited, although more compared to the high-frequency excitation (T=0.1 s), and it is essentially verified that the longer the lengths, the larger the failure displacements. In fact, the total maximum for a column length value of 3.8 meters indicates a fairly flexible structure. Therefore, it is estimated that here we have resonance of the structure. The network prediction for a relatively low-frequency excitation (T=1 s) gives values for the maximum failure velocity between 0.5 and 2.5 m/s. The maximum values are found at the largest values of column length. The curve is not truly monotonic. However, the minimum values are found at the smallest values of column length. Therefore, in principle, stiffer columns are more likely to have a reduced maximum velocity. The network prediction for a relatively low-frequency excitation (T=1 s) gives values for the maximum failure acceleration between 20 and 150 m/s². It is noted that these displacements are nodal and point-

like, so they may have an increased value. In fact, these are located spatially slightly lower than the top of the columns. The maximum values are achieved when the height of the frame, i.e., the columns, is 4 m. Therefore, for a flexible structure, the predictions are maximized. This is a result of the resonance because the flexible structure has a high eigenperiod value, as does the excitation.

Subsequently, the models proposed are accurate and reliable in terms of the supervised learning. A strong correlation of outputs and targets is attained. The physical constraints of the model are evident in the proposed model. Moreover, it can be adjusted with an alleviated amount of computational time. Thus, it can be a computational and numerical tool to assist earthquake engineering design, as it can give reliable predictions of the failure attributes of a one-story building. The increased reliability of the failure analysis as a consequence of the fiber beam force-based element leads to a significant accuracy of the proposed machine learning model. Finally, it can be observed that the total amount of the values selected for the beams is realistic, and since the generality of the model is attained, as a consequence of no overfitting, one can provide estimations even outside of the range of the input training dataset. The coherence of the proposed modeling is practical for engineers and practitioners, and therefore, an estimation tool for the seismic design is available through the present model.

7. Conclusions

In this work, a model that estimates the main parameters at failure of a single-story building subjected to a horizontal dynamic load is presented. The model is formulated through a Feed-Forward Neural Network architecture. The horizontal dynamic load is sinusoidal with an excitation period equal to the structure's eigenperiod. The input parameters of the model are the frame height H, the frame length L, the Young Modulus E, the yield stress σ_y , and the eigenperiod of the structure T. The output parameters of the model are the failure load P_0 , the time of the failure t_0 , the maximum displacement d_{max} of the frame at failure, the corresponding maximum velocity v_{max} , and the corresponding maximum acceleration a_{max} . After the construction of the dataset matrix, through dynamic failure time history analysis of a single-story building, a neural network model was obtained with the aid of the MATLAB neural network toolbox. Two hidden layers with 64 Neurons each were selected as the architecture. The activation functions are the sigmoid function for all layers except the output layer, and the pure linear to the output layer. The error metric was the Mean Squared Error (MSE), and the early stopping was employed to avoid overfitting.

In all subsets and in the total dataset matrix, it has been proven that the model could estimate the outputs with substantial accuracy in relation to the given targets. Slight underestimations of the proposed model are given through the proposed machine learning formulation. The failure time in all cases was small enough and did not provide time for the residents of the infrastructure to evacuate it. Failure loads are about 10-50 kN, which could resemble a force of intermediate magnitude as it corresponds to a mass load of 1-5 Mgr. The failure peak displacements are substantially high, about 5 cm, and this results in an inter-story drift of the order of magnitude of 1-2%, which corresponds to a smaller value than the corresponding regulatory maximum allowed drift for avoiding structural collapse, which in EC8 is 10%. The failure peak velocity is in the vicinity of 1-2 m/s, which is an intermediate value of velocity. In addition, the peak value accelerations, which are nodal values in the places near the top tip, are about 150 m/s², which is considered very high. These values can be justified as follows. When a fiber fails, the loads of stiffness are practically zero. Therefore, the total balance could only be achieved from inertia and damping forces. Damping forces are relatively low; subsequently, the majority of the forces are the inertia counterpart. Thus, the accelerations are increased. In terms of a practical engineering point of view, the present formulation depicts that the failure time is far smaller than a second. That results in the increased probability of having casualties. This probability is proven not to be very different when the stiffness of the structure alters. Since the structures were excited to have a resonance, it is important to highlight that this case is the critical rather than the actual value of the eigenperiod. It is evident that the increase in ductility of the structure would increase the failure time, thus it is highlighting the importance of regulatory proposals for ductility. Finally, it is shown through our results that the majority of the output parameters are influenced by the ratio of the stiffness of the beams to the columns rather than the stiffnesses alone. A stiffer behavior is obtained when the ratio

tends to zero, which means the columns are stronger than the beams. This is expected, and it is reliably quantified through the proposed modeling.

The proposed machine learning framework presents the following setbacks and disadvantages. The first one is that no comparison or training with experimental data was performed. That would increase the model's reliability. However, the amount of reliability with the present data is substantial, and the finite element modeling is proven reliable through the respective literature of fiber beam force-based elements. Moreover, the analyses could employ more material characteristic values of different orders of magnitude, such as the reinforced concrete usual value for E=30 GPa. Finally, the analyses with more complex structures, such as multistory buildings with non-uniform material law to all beam elements, and the subsequent comparison with the present findings should be implemented. As future work, an investigation of the present geometry and horizontal load, with time function pulse forces, such as T-Ricker pulse, would add to the present literature about the estimation of dynamic loading failure to pulse forces, which are also often present in structures after earthquakes. Additionally, an investigation of other machine learning frameworks could be used in order to construct more detailed models, such as the method of SHapley Additive exPlanations (SHAP) [24] or convolutional autoencoders [33].

References

- [1] Elenas A. Athens earthquake of 7 September 1999: Intensity measures and observed damages. ISET J Earthq Technol. 2003;40(1):77–97.
- [2] Dedeoglu IO, Yetkin M, Tunc G, Ozbulut OE. Evaluating earthquake-induced damage in Doğanşehir, Malatya after 2023 Kahramanmaraş earthquake sequence: Geotechnical and structural perspectives. J Build Eng. 2025;112266. https://doi.org/10.1016/j.jobe.2025.112266
- [3] Laosunthara A, Saengtabtim K, Suppasri A, Leelawat N, Ohashi T. Disaster management in a shrinking society: The 2024 Noto Peninsula earthquake's holiday shutdown, challenges and lessons learned. Int J Disaster Risk Reduct. 2025;125:105582. https://doi.org/10.1016/j.ijdrr.2025.105582
- [4] Ozmen HB, Yalçıner Çal D. The economic impact of earthquakes: A global assessment of direct and indirect losses. J Res Design. 2025. https://doi.org/10.17515/rede2025-007en0716rs
- [5] Liu Z, Ma X, Zhang H, Song Q, Chen Y, Ma C. Seismic response characteristics of subway stations in the Jinan area: An experimental and computational approach. J Earthq Eng. 2025. https://doi.org/10.1080/13632469.2025.2484588
- [6] Qayoumi AS, Shalizi H, Dhankot MA. Review on artificial intelligence application in structural earthquake engineering. Int J Sci Res Arch. 2025;14(1):83–92. https://doi.org/10.30574/ijsra.2025.14.1.2659
- [7] Naderpour H, Akbari M, Mirrashid M, Kontoni DPN. Compressive capacity prediction of stirrup-confined concrete columns using neuro-fuzzy system. Buildings. 2022;12(9):1386. https://doi.org/10.3390/buildings12091386
- [8] Arora HC, Kumar S, Kontoni DPN, Kumar A, Sharma M, Kapoor NR, Kumar K. Axial capacity of FRP-reinforced concrete columns: Computational intelligence-based prognosis for sustainable structures. Buildings. 2022;12(12):2137. https://doi.org/10.3390/buildings12122137
- [9] Rezazadeh Eidgahee D, Soleymani A, Hasani H, Kontoni DPN, Jahangir H. Flexural capacity estimation of FRP reinforced T-shaped concrete beams via soft computing techniques. Comput Concr. 2023;32(1):1–13. https://doi.org/10.12989/cac.2023.32.1.001
- [10] Onyelowe KC, Kontoni DPN, Pilla SRM, Hanandeh S, Ebid AM, Razzaghian Ghadikolaee M, Stephen LU. Runtime-based metaheuristic prediction of the compressive strength of net-zero traditional concrete mixed with BFS, FA, SP considering multiple curing regimes. Asian J Civ Eng. 2023;25:1241–53. https://doi.org/10.1007/s42107-023-00839-3
- [11] Onyelowe KC, Jagan J, Kontoni DPN, Moghal AAB, Onuoha IC, Viswanathan R, Soni DK. Utilization of GEP and ANN for predicting the net-zero compressive strength of fly ash concrete toward carbon neutrality infrastructure regime. Int J Low-Carbon Technol. 2023;18:902–14. https://doi.org/10.1093/ijlct/ctad081
- [12] Mirrashid M, Naderpour H, Kontoni DPN, Jakubczyk-Gałczyńska A, Jankowski R, Nguyen TN. Optimized computational intelligence model for estimating the flexural behavior of composite shear walls. Buildings. 2023;13(9):2358. https://doi.org/10.3390/buildings13092358
- [13] Annamdasu ML, Challagulla SP, Kontoni DPN, Rex J, Jameel M, Vicencio F. Artificial neural network-based prediction model of elastic floor response spectra incorporating dynamic primary-secondary structure interaction. Soil Dyn Earthq Eng. 2024;177:108427. https://doi.org/10.1016/j.soildyn.2023.108427

- [14] Naderpour H, Abbasi M, Kontoni DPN, Mirrashid M, Ezami N, Savvides AA. Integrating image processing and machine learning for the non-destructive assessment of RC beams damage. Buildings. 2024;14(1):214. https://doi.org/10.3390/buildings14010214
- [15] Chang S, Arora HC, Kumar A, Kontoni DPN, Kumar P, Kapoor NR, Singh J. Estimation of confined compressive strength of LRS-FRP concrete specimens with computational intelligence. ZAMM J Appl Math Mech. 2024;104:e202400455. https://doi.org/10.1002/zamm.202400455
- [16] Vishnupriyan M, Kontoni DPN, Onyelowe KC, Nakkeeran G, Vishal M, Premkumar G, Selvakumar A. Experimental and ANN analysis of cold-formed steel build-up columns with and without intermediate web stiffeners under axial compression. J Struct Design Constr Pract (ASCE). 2025;30(3):04025048. https://doi.org/10.1061/JSDCCC.SCENG-1751
- [17] Salem NM, Kontoni DPN, Deifalla AF, Savvides AA. A machine learning model for predicting the shear strength of slender FRP-reinforced concrete elements. J Eng Sci Technol Rev. 2025;18(1):48–56. http://dx.doi.org/10.25103/jestr.181.06
- [18] Sheik M, Kontoni DPN, Anandh S, Sindhu Nachia S. Parametric FEM analysis of cellular composite steel-concrete beams and deflection prediction using least squares support vector machine optimized with metaheuristic algorithms. J Struct Design Constr Pract (ASCE). 2026;31(1):04025112. https://doi.org/10.1061/ISDCCC.SCENG-1756
- [19] Parthasarathi N, Prakash M, Kontoni DPN. Assessing failure mechanisms in reinforced concrete frame structures under thermo-mechanical loading using finite element analysis. Asian J Civ Eng. 2025;26:3289–315. https://doi.org/10.1007/s42107-025-01374-z
- [20] Raissi M, Perdikaris P, Karniadakis GE. Physics-informed neural networks: A deep learning framework for solving forward and inverse problems involving nonlinear partial differential equations. J Comput Phys. 2019;378:686–707. https://doi.org/10.1016/j.jcp.2018.10.045
- [21] Kutyłowska M. Neural network approach for failure rate prediction. Eng Fail Anal. 2015;47:41–8. https://doi.org/10.1016/j.engfailanal.2014.10.007
- [22] Chatterjee S, Sarkar S, Hore S, Dey N, Ashour AS, Balas VE. Particle swarm optimization trained neural network for structural failure prediction of multistoried RC buildings. Neural Comput Appl. 2017;28(8):2005–16. https://doi.org/10.1007/s00521-016-2190-2
- [23] Tian L, Noore A. Evolutionary neural network modeling for software cumulative failure time prediction. Reliab Eng Syst Saf. 2005;87(1):45–51. https://doi.org/10.1016/j.ress.2004.03.028
- [24] Zhao X. A SHAP algorithm-based prediction of the interlaminar shear strength degradation of G/BFRP bars embedded in concrete exposed to marine environment. Case Stud Constr Mater. 2025;22:e04770. https://doi.org/10.1016/j.cscm.2025.e04770
- [25] Zhao X. Prediction of interlaminar shear strength retention of FRP bars in marine concrete environments using XGBoost model. J Build Eng. 2025;105:112466. https://doi.org/10.1016/j.jobe.2025.112466
- [26] Zhang PF, Zhang D, Zhao XL, Iqbal M, Zhao X, Zhao Q. Natural language processing-based deep transfer learning model across diverse tabular datasets for bond strength prediction of composite bars in concrete. Comput-Aided Civ Infrastruct Eng. 2025;40(7):917–39. https://doi.org/10.1111/mice.13357
- [27] Zhang Z, Liu Q, Wu D. Predicting stress–strain curves using transfer learning: Knowledge transfer across polymer composites. Eng Appl Artif Intell. 2025;112:112011. https://doi.org/10.1016/j.engappai.2025.112011
- [28] Ramesh V, Pandulu G, Khanam N, Lian OC. Compressive strength prediction of ecofriendly recycled aggregate concrete: A machine learning approach. Res Eng Struct Mater. 2025. https://doi.org/10.17515/resm2025-595me1212rs
- [29] Spacone E, Filippou FC, Taucer FF. Fibre beam-column model for non-linear analysis of R/C frames: Part I. formulation. Earthq Eng Struct Dyn. 1996;25:711–25. https://doi.org/10.1002/(SICI)1096-9845(199607)25:7 <a href="https://doi.org/10.1002/(SICI)109607]25:7 <a href="https://doi.org/10.1002/(SICI)109607/(SICI)109607/(SICI)109607/(SICI)1096
- [30] Cybenko G. Approximation by superpositions of a sigmoidal function. Math Control Signals Syst. 1989;2(4):303–14. https://doi.org/10.1007/BF02551274
- [31] Hendrycks D, Gimpel K. Gaussian error linear units (GELUs). arXiv [Preprint]. 2016. Available from: https://arxiv.org/abs/1606.08415
- [32] Opschoor JAA, Schwab C. Deep ReLU networks and high-order finite element methods II: Chebyšev emulation. Comput Math Appl. 2024;169:142–62. https://doi.org/10.1016/j.camwa.2024.06.008
- [33] Masci J, Meier U, Ciresan D, Schmidhuber J. Stacked convolutional auto-encoders for hierarchical feature extraction. In: Int Conf Artif Neural Netw. 2011; p. 52–9. https://doi.org/10.1007/978-3-642-21735-7 7